

Research

Open Access

Predicting the protein-protein interactions using primary structures with predicted protein surface

Darby Tien-Hao Chang*, Yu-Tang Syu and Po-Chang Lin

Address: Department of Electrical Engineering, National Cheng Kung University, Tainan, 70101, Taiwan

E-mail: Darby Tien-Hao Chang* - darby@ee.ncku.edu.tw; Yu-Tang Syu - n2696195@mail.ncku.edu.tw;

Po-Chang Lin - n2697193@mail.ncku.edu.tw

*Corresponding author

from The Eighth Asia Pacific Bioinformatics Conference (APBC 2010)
Bangalore, India 18-21 January 2010

Published: 18 January 2010

BMC Bioinformatics 2010, 11(Suppl 1):S3 doi: 10.1186/1471-2105-11-S1-S3

This article is available from: <http://www.biomedcentral.com/1471-2105/11/S1/S3>

© 2010 Chang et al; licensee BioMed Central Ltd.

This is an open access article distributed under the terms of the Creative Commons Attribution License (<http://creativecommons.org/licenses/by/2.0>), which permits unrestricted use, distribution, and reproduction in any medium, provided the original work is properly cited.

Abstract

Background: Many biological functions involve various protein-protein interactions (PPIs). Elucidating such interactions is crucial for understanding general principles of cellular systems. Previous studies have shown the potential of predicting PPIs based on only sequence information. Compared to approaches that require other auxiliary information, these sequence-based approaches can be applied to a broader range of applications.

Results: This study presents a novel sequence-based method based on the assumption that protein-protein interactions are more related to amino acids at the surface than those at the core. The present method considers surface information and maintains the advantage of relying on only sequence data by including an accessible surface area (ASA) predictor recently proposed by the authors. This study also reports the experiments conducted to evaluate a) the performance of PPI prediction achieved by including the predicted surface and b) the quality of the predicted surface in comparison with the surface obtained from structures. The experimental results show that surface information helps to predict interacting protein pairs. Furthermore, the prediction performance achieved by using the surface estimated with the ASA predictor is close to that using the surface obtained from protein structures.

Conclusion: This work presents a sequence-based method that takes into account surface information for predicting PPIs. The proposed procedure of surface identification improves the prediction performance with an *F-measure* of 5.1%. The extracted surfaces are also valuable in other biomedical applications that require similar information.

Background

The different types of interactions among proteins are essential to various biological functions in a living cell. Information about these interactions provides a basis to construct protein interaction networks and improves our understanding of the general principles of the functioning of biological systems [1]. Recent years have seen the development of various experimental techniques for systematic protein-protein interaction (PPI) analysis [2-5]. At present, however, experimentally detected interactions represent only a small fraction of the real interaction network [6,7]. Therefore, a number of computational approaches have been proposed to expedite the PPI detection process based on only experimental techniques [8].

Computational methods that depend on not only sequence information but also some prior knowledge of, for example, localization data [9], structural data [10,11], expression data [12,13] or information on the interactions of orthologs [14,15] cannot be applied on some essential proteins that are observed in most organisms [16]. To solve this problem, several sequence-based algorithms have been developed to detect potentially interacting protein pairs when no auxiliary information is available [17-23].

This work presents a novel sequence-based method which involves a mechanism for identifying the protein surface to help PPI prediction. This method employs the conjoint triad feature [24] for describing protein sequences and the relaxed variable kernel density estimator (RVKDE) [25] for classification. Conjoint triads, which treat three continuous amino acids as a single unit, have been shown to be a useful set of features in predicting protein-protein interactions [24]. This work improves this feature set by focusing on conjoint triads at the protein surface. This improvement is based on the assumption that protein-protein interactions are more related to amino acids at the surface than those at the core. To maintain the advantage of depending on only sequence information, this method employs an accurate accessible surface area (ASA) predictor, recently proposed by the authors [26], to determine the protein surface.

In this study, a collection of 691 PPIs is used to evaluate the prediction performance with and without the proposed mechanism for identifying the protein surface. The experimental results show that the surface information promotes PPI prediction based on feature encoding with conjoint triads. Furthermore, the quality of the predicted surface is analyzed using a number of protein structures collected from the Protein Data Bank (PDB) [27]. The experimental results demonstrate that the

performance of PPI prediction achieved using the predicted surface is close to that achieved using the surface obtained from protein structures.

Results and discussion

This section first describes the workflow of the proposed method. Next, the measurements and datasets for performance evaluation are presented. The proposed method is evaluated and compared with another sequence-based PPI predictor. At the end of the section, the predicted surface is compared to those obtained from protein structures.

Proposed PPI prediction scheme

Figure 1 depicts the workflow of the developed method. Steps marked with an asterisk indicate the major differences between the procedure in this work and those presented in previous PPI studies. First, the feature vectors of both proteins of a given protein pair are individually generated. This operation is further split into three steps: 'ASA Prediction', 'Surface Identification' and 'Feature Encoding'. The 'ASA Prediction' step invokes a sequence-based ASA predictor for assigning a relative ASA (RSA) value to each residue of the protein sequence. Based on these RSA values, the 'Surface Identification' step identifies surface sequence segments in which most residues have large RSA values. The detailed criterion of identifying surface segments is presented in the Methods section. Next, the 'Feature Encoding' step determines the frequencies of conjoint triads that are observed in the identified surface segments and uses these frequencies to generate the feature vector. Finally, the two feature vectors of the given protein pair are concatenated and sent to RVKDE for classifying whether the two proteins have interactions. See the Methods section for details of all of these steps.

Measurements

Determining whether two proteins have interactions is a binary classification problem. Table 1 lists five measurements that are applied widely on evaluating binary classification problems. The *accuracy* is the most commonly used measurement, which represents an overall performance of a predictor. The *F-measure* is designed for problems where a class of instances attracts most attention, which is appropriate for PPI prediction [28]. The *precision* is the fraction of predicted interacting protein pairs that truly have interactions. The *sensitivity* is the fraction of interacting protein pairs correctly predicted to have interactions, while the *specificity* is the fraction of non-interacting protein pairs correctly predicted to have no interaction.

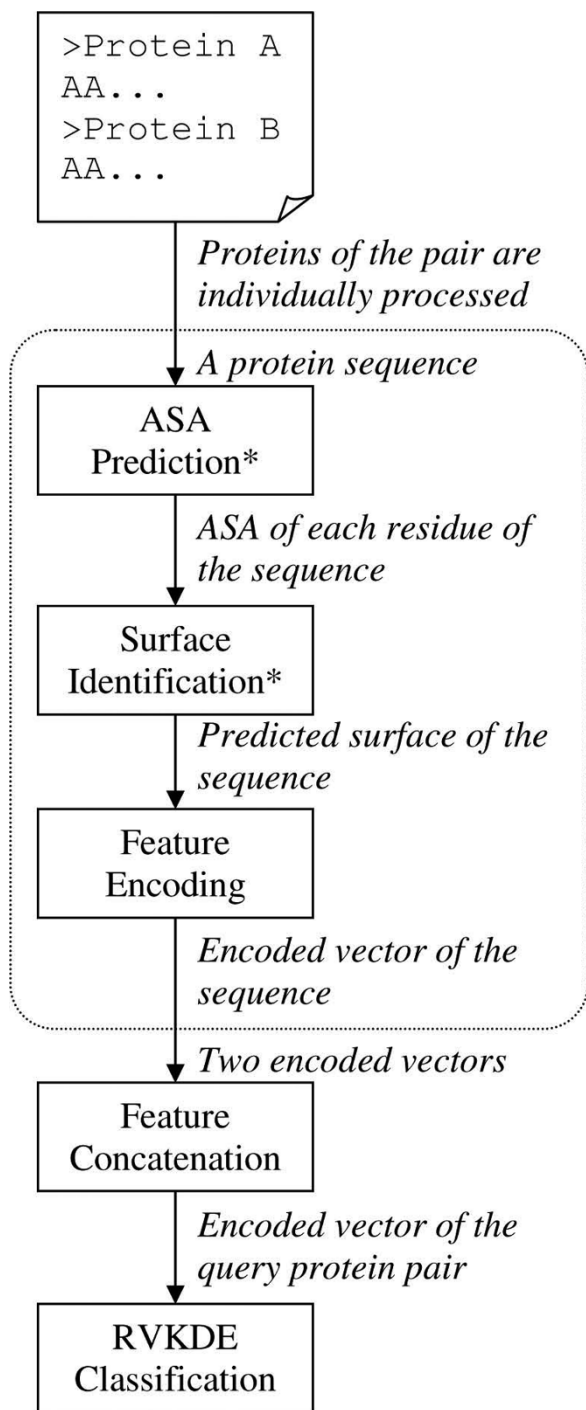


Figure 1
Workflow of proposed method to predict interacting protein pairs. Given a pair of protein sequences, this method first encodes each of the two sequences as a vector. The encoding process comprises three steps; the two steps marked with an asterisk are the major contributions of this work. The two vectors are concatenated as the feature vector of the protein pair and submitted to the RVKDE for classifying whether the two proteins have interactions.

Table 1: Evaluation measurements

Measurement	Abbreviation	Equation
Accuracy	Acc.	$(TP+TN)/(TP+TN+FP+FN)$
F-measure	Fm.	$2TP/(2TP+FP+FN)$
Precision	Prec.	$TP/(TP+FP)$
Sensitivity (recall)	Sens.	$TP/(TP+FN)$
Specificity	Spec.	$TN/(TN+FP)$

The definitions of the abbreviations used: TP is the number of interacting protein pairs correctly classified; FN is the number of interacting protein pairs incorrectly classified as non-interacting; TN is the number of non-interacting protein pairs correctly classified; and FP is the number of non-interacting protein pairs incorrectly classified as interacting.

Datasets

A challenge in preparing protein-protein interaction datasets is the presence of some interactions that are observed in the laboratory experimentation but do not occur physiologically [6]. To ensure the quality of PPI data, an interaction should be consistent with other types of information [29], such as metabolomic [30] and gene-gene relationship data [31]. Though these types of data are often incomplete in most organisms at present, the interaction network of transcription factors (TF) of *Saccharomyces cerevisiae* is an extensively studied system in which all of such information are currently available [29]. Therefore, this study collects 691 interactions of 211 yeast TFs from several studies and databases [32-36] to generate a PPI dataset, SC691. In this dataset, the 691 interactions are used as positive instances, while other protein pairs created by coupling the 211 TFs are used as negative instances.

Evaluation of PPI prediction

In the experiment, the SC691 dataset is randomly split into three subsets of 341, 175 and 175 interacting pairs. These subsets also contain 341, 175 and 175 non-interacting pairs obtained by arbitrarily sampling of the negative instances in the SC691 dataset. Care is taken to ensure that different subsets will not share identical instances. In this experiment, the first subset is used as the training set to predict the other two subsets. The predicted results of the second subset are used for parameter selection, while the predicted results of the third subset indicate the prediction performance of a PPI predictor. Therefore, an evaluation process is performed by first using the first subset to predict the second subset. Then the parameters that maximize the F-measure are used to predict the third subset. Since the procedure for generating these subsets involves randomness, the evaluation process is performed ten times to eliminate the evaluation bias in a single evaluation process.

Table 2 presents the prediction performance of the proposed method under various surface conditions. In

Table 2: Performance achieved by considering and by neglecting surface information

	Acc. (%)	Fm. (%)	Prec. (%)	Sens. (%)	Spec. (%)
Without surface information					
Shen <i>et al.</i> 's work	68.2 ± 4.3	70.4 ± 3.2	66.4 ± 5.1	75.4 ± 5.4	61.0 ± 10.2
Surface identified using different σ					
1	72.3 ± 1.4	73.7 ± 1.6	70.3 ± 2.3	77.8 ± 4.4	66.9 ± 5.1
2	72.1 ± 3.2	74.0 ± 2.2	69.7 ± 4.2	79.3 ± 3.7	64.9 ± 8.3
3	74.1 ± 2.0	75.5 ± 2.0	71.8 ± 2.4	79.7 ± 3.5	68.6 ± 4.0
4	71.7 ± 3.8	73.4 ± 2.3	69.8 ± 4.9	77.9 ± 5.9	65.4 ± 11.5

Parameter σ restricts the minimum number of surface residues in a surface sequence segment.

this work, the predicted surface is union of several surface sequence segments of fixed length. The parameter σ restricts the minimum number of surface residues in a surface segment, and thereby affects the predicted surface. See the 'Surface identification' subsection for details. Table 2 also includes the prediction performance of the sequence-based method proposed by Shen *et al.* [24], which uses conjoint triads that are observed in protein sequences without considering surface information. In Table 2, all the five measurements of are improved after introducing the surface information without depending on the surface condition. Considering surface segments that include at least three surface residues achieves the best performance, and the other three surface conditions deliver similar performance. This suggests that to form a stable interface requires at least three residues. Restricting that a surface segment must have at least four surface residues would be too rigorous and filter out some potential surface segments.

As a result, the average *Acc.*, *Fm.*, *Prec.*, *Sens.* and *Spec.* of the developed method are 74.1%, 75.5%, 71.8%, 79.7% and 68.6%, respectively. All five measurements are superior to those delivered by the predictor without surface information. These results show that the proposed mechanism for identifying the protein surface helps to predict protein-protein interactions based on feature encoding with conjoint triads.

Evaluation of predicted surface

As shown in Figure 1, the 'ASA Prediction' and 'Surface Identification' steps are the major differences between this work and others. To evaluate the added components, this subsection reports the experiment for answering two questions: a) how the predicted surface overlap with the surface obtained from protein structures and b) how the PPI prediction performs when using the predicted surface compared to those using the surface obtained from protein structures. The ten TFs from the SC691 dataset that have structures in PDB (Table 3) are used to generate a smaller dataset. This dataset, called SC85, includes 85 positive and 1980 negative instances from the SC691 dataset. Each pair of the SC85 dataset

Table 3: Proteins in the SC691 dataset that have structures in PDB

Name	Description	PDB ID: chain
SPT4	Transcription initiation protein	2EXU:A
GAL80	Galactose/lactose metabolism regulatory protein	3BTY:A
MED18	RNA polymerase II mediator complex subunit 18	2HZM:B
MED20	RNA polymerase II mediator complex subunit 20	2HZM:A
MED21	RNA polymerase II holoenzyme component SRB7	1YKE:B
MTF1	Mitochondrial replication protein	114W:A
NHP6A	Nonhistone protein 6A	1CG7:A
PHO80	Cyclin, negatively regulates phosphate metabolism	2PMI:B
TOA1	Transcription initiation factor IIA large chain	1RMI:C
TOA2	Transcription initiation factor IIA small chain	1RMI:B

contains at least one of the ten TFs. In this experiment, a prediction is made by five-fold cross validation of the SC85 dataset, in which each fold includes 17 positive and 396 negative instances. The cross validation is performed ten times to eliminate the evaluation bias. The surface condition is set to consider surface segments that include at least three surface residues.

Table 4 shows the overlap of the predicted surface and the surface obtained from protein structures, called 'structural surface', in the residue level. The predicted surface is identified based on the predicted ASA obtained from the adopted ASA predictor, while the structural surface is identified based on the actual ASA obtained by invoking the Dictionary of Protein Secondary Structure (DSSP) program [37]. In this experiment, at least 75% (91.9% in average) of surface residues-residues in the structural surface-are included in the predicted surface. Conversely, some individual trials delivered <60% *specificity*, and the average *specificity* (77.7%) is relative lower in comparison with the *sensitivity*. These results indicate that a certain percentage of buried residues-residues outside the structural surface-are incorrectly included in the predicted surface. Namely, the proposed method delivers a larger surface than that obtained based on actual ASA. Overall, the predicted surface is consistent to structural surface in this dataset according to the *accuracy* and *F-measure*.

Table 4: Overlap between predicted and structural surface

	Acc. (%)	Fm. (%)	Prec. (%)	Sens. (%)	Spec. (%)
Trial 1	76.1	81.3	76.0	87.3	59.7
Trial 2	76.3	81.2	71.1	94.5	54.9
Trial 3	78.6	82.3	74.2	92.5	62.3
Trial 4	77.2	81.3	83.3	79.4	73.7
Trial 5	95.1	96.2	92.7	100.0	86.9
Trial 6	88.0	90.2	82.2	100.0	73.3
Trial 7	95.1	96.2	92.7	100.0	86.9
Trial 8	95.1	96.2	92.7	100.0	86.9
Trial 9	83.0	83.1	92.4	75.4	92.4
Trial 10	93.4	94.7	100.0	90.0	100.0
Overall	85.8 ± 8.4	88.3 ± 7.0	85.7 ± 9.7	91.9 ± 9.0	77.7 ± 15.2

The equation of each measurement is identical to Table 2, while the definitions of the abbreviations used are different: TP is the number of residues within the structural surface and are correctly included in the predicted surface; FN is the number of residues within the structural surface but are incorrectly excluded from the predicted surface; TN is the number of residues outside the structural surface and are correctly excluded from the predicted surface; and FN is the number of residues outside the structural surface but are incorrectly included in the predicted surface.

The next analysis aims to elaborate how much does the difference between predicted and structural surface affect the results of PPI prediction. Table 5 presents the performance of PPI prediction using the predicted and structural surface. Though the predicted surface performs worse than the structural surface, the differences in all evaluation measures are less than the standard deviations of using the structural surface. These results reveal that the added components of this work can achieve comparable performance of dealing yeast TFs to that delivered using structure information.

In the end of this section, a protein pair from the collected 691 PPIs of which both the proteins appear in the same complex structure in PDB is used to plot the overlap between the predicted surface and the interface. This complex (PDB ID: 2HZM) includes the two subunits (Med18 and Med20) of the RNA polymerase II, which is central to eukaryotic gene expression and has been studied extensively [38]. Figure 2 presents the interface residues of Med18 (chain B in 2HZM) and Med20 (chain A in 2HZM). Interface residues are defined as those that have at least one heavy atom within 5 Å

Table 5: Performance achieved using predicted and structural surface

	Acc. (%)	Fm. (%)	Prec. (%)	Sens. (%)	Spec. (%)
Predicted surface					
Trial 1	96.2	38.1	58.5	28.2	99.1
Trial 2	96.2	40.9	57.4	31.8	99.0
Trial 3	96.1	38.2	54.3	29.4	98.9
Trial 4	96.3	38.7	61.5	28.2	99.2
Trial 5	96.6	40.3	70.6	28.2	99.5
Trial 6	96.4	43.1	62.2	32.9	99.1
Trial 7	96.7	41.0	75.0	28.2	99.6
Trial 8	96.4	40.9	61.9	30.6	99.2
Trial 9	94.7	37.5	36.3	38.8	97.1
Trial 10	95.7	39.7	47.5	34.1	98.4
Overall	96.1 ± 0.6	39.8 ± 1.7	58.5 ± 11.0	31.1 ± 3.5	98.9 ± 0.7
Structural surface					
Trial 1	96.0	39.7	52.9	31.8	98.8
Trial 2	96.6	41.3	69.4	29.4	99.4
Trial 3	96.1	40.3	55.1	31.8	98.9
Trial 4	96.3	39.7	61.0	29.4	99.2
Trial 5	96.3	40.3	59.1	30.6	99.1
Trial 6	96.4	42.7	60.9	32.9	99.1
Trial 7	96.2	41.5	56.0	32.9	98.9
Trial 8	96.5	42.5	64.3	31.8	99.2
Trial 9	95.9	38.8	50.0	31.8	98.6
Trial 10	96.0	40.3	51.9	32.9	98.7
Overall	96.2 ± 0.2	40.7 ± 1.3	58.1 ± 6.0	31.5 ± 1.3	99.0 ± 0.3

ASA values of predicted surface are obtained from the adopted ASA predictor. ASA values of structural surface are obtained using the DSSP program.

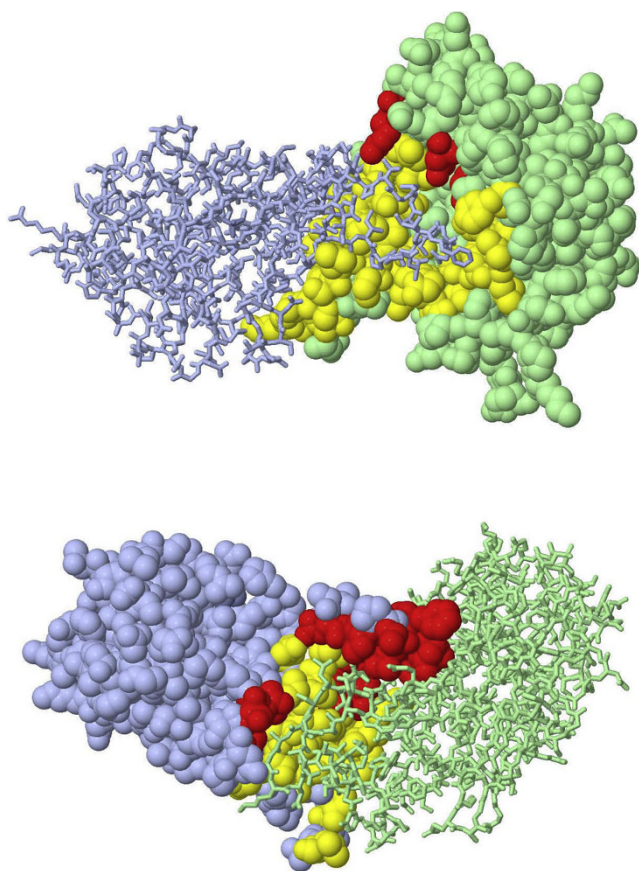


Figure 2
Example of the surface predicted by the present method. This example employs the two subunits of RNA polymerase II (PDB ID: 2HZM), Med18 (chain B) and Med20 (chain A), to show the predicted surface relative to the interface residues. The protein chain in *spacefill* mode is the target subunit used in surface identification; the protein chain that is displayed in *stick* mode is treated as the interacting partner of the target subunit. The predicted surface that overlaps the interface residues is shown in yellow, and the non-overlapping region is shown in red. Med18 is the target subunit in (a), and Med20 is the target subunit in (b).

distance of the interacting partner. This definition is similar to those used in many studies [39-41].

For Med18, the present method successfully excludes 80 (accounting for ~26.1%) from total 307 residues while preserving 48 (accounting for ~92.3% of the 52) interface residues. As shown in Figure 2(a), most interface residues, specified in yellow, are included. However, for Med20, the proposed method misses 24 (accounting for ~54.5% of the 44) interface residues in the predicted surface in Figure 2(b). Figure 2(b) reveals that the predicted surface misses the segment (residues 86-107) of Med20 that acts like an arm stretching to Med18. A

comparison with the interface shown in Figure 2(a) suggests that the present method may perform better at handling flatter interfaces. Since protein subunits may interact and form relatively flat or twisted surfaces [42], the good performance of the present method probably results from the fact that most of the collected *S. cerevisiae* TFs have relatively flat surfaces.

These results also reveal that the proposed mechanism for identifying the surfaces of proteins with relatively twisted surfaces must be improved.

Conclusion

An enormous gap exists between the number of protein structures and the huge number of protein sequences. Hence, predicting protein functions directly from amino acid sequences remains one of the most important problems in life science. This work presents a computational approach for PPI prediction based on only sequence information. Notably, a mechanism of extracting surface information is proposed to refine the feature vector for representing a protein sequence. This method is analyzed in terms of a) the performance in predicting PPIs and b) the quality of the predicted surface. The experimental results show that the present method improves on the prediction performance of PPI with an *F-measure* of 5.1%. Furthermore, the predicted surface of yeast TFs is consistent with that obtained from structures, which encourages applying the present steps of surface identification in other biomedical problems that require similar information.

Methods

ASA prediction

This study adopts two cascading regressions to predict relative ASA (RSA) values. The first stage uses the PSSM-2SP (stands for position specific scoring matrix with two sub-properties) profile [26] to encode a protein sequence. The PSSM-2SP profile is an enhanced PSSM profile, which describes the likelihood of a particular residue substitution at a specific position based on evolutionary information [21]. The construction of the PSSM profile is achieved by first invoking the PSI-BLAST program [43] to the non-redundant (NR) database obtained from the NCBI. The PSSM-2SP profile adds more two accumulated profile values according to residue groups *Charged_{sel}* (K and D) and *Tiny_{sel}* (A and G). The resulting PSSM-2SP profile is rescaled to [0,1], using the following logistic function [44]:

$$x' = \frac{1}{1 + \exp(-x)},$$

where x is the raw value in the PSSM profile and x' is the value corresponding to x after rescaling. Finally, we add a

terminal flag and format the profile into the vector representation with a window size w_1 ($w_1 = 11$ in our implementation). Figure 3 shows an example of encoding a residue to its corresponding PSSM-2SP form.

The second stage encodes a protein sequence based on neighboring solvent accessibility [26,45]. The i -th residue in a protein sequence is represented as a $2w_2+1$ dimensional vector $\mathbf{v} = (a_{i-h}, t_{i-h}, a_{i-h+1}, t_{i-h+1}, \dots, a_i, t_i, \dots, a_{i+h}, t_{i+h}, l)$, where a_i is the predicted RSA value of the i -th residue in the first regression, t_i is the terminal flag as either 1 (a null/terminal residue) or 0 (otherwise), l is the sequence length and $w_2 = 2h+1$ is window size ($w_2 = 5$ in our implementation).

The support vector regression (SVR) is used as the regression tool for both stages. The SVR is a kernel regression technique that constructs a model based on support vectors. This model expresses γ as a function of \mathbf{v} with several parameters:

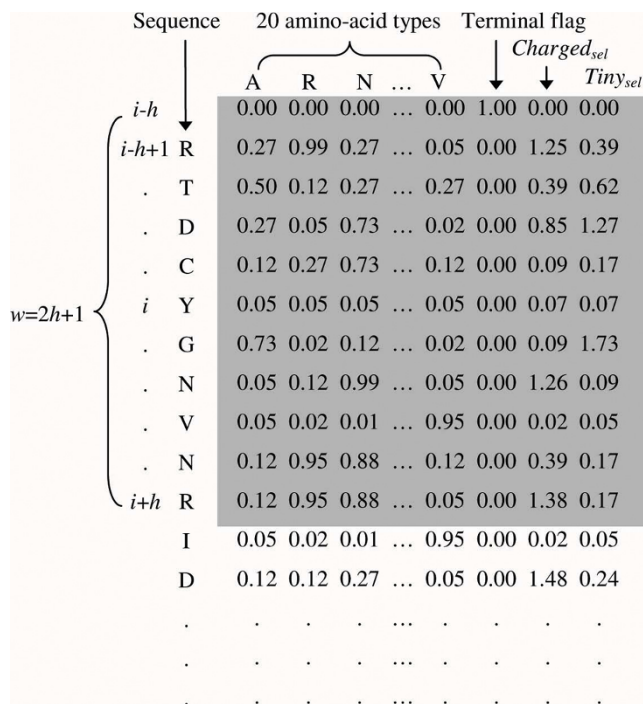


Figure 3
Example of encoding a residue in the PSSM-2SP form. This example encodes the fifth residue ($i = 5$) of a protein (PDB ID: 154L) with window size 11 ($w = 11$ and $h = 5$). A position is represented by a 23-dimensional vector (20 amino acid values, a terminal flag and two group values). The first row is a pseudo terminal residue where only the terminal flag is 1 and all 22 other values are zero. Finally, the i -th residue is encoded with its neighboring positions to form a 253-dimensional feature vector.

$$y = b + \sum_{s_i \text{ is a support vector}} w_i K(\mathbf{v}, \mathbf{s}_i),$$

where $K()$ is the kernel function, and b and w_i are numerical parameters determined by minimizing the prediction error on training samples. The problem is to find the support vectors and determine parameters b and w_i , which can be solved by constrained quadratic optimization [46]. The LIBSVM package (version 2.86) [47] is used for SVR implementation in this study.

Surface identification

The employed ASA predictor makes predictions at the residue level. The predicted RSA value of each residue enables surface residues to be defined as those whose RSA values are equal to or larger than a threshold t . These identified surface residues are frequently scattered throughout the protein sequences. This work develops a process for generating a set of surface segments each of which is a consecutive sub-sequence of minimum length. Because a conjoint triad represents three continuous amino acids, these consecutive segments are more suitable than scattered surface residues for being encoded with conjoint triads.

Figure 4 depicts the process of surface identification. The present method uses a sliding window of size w to scan

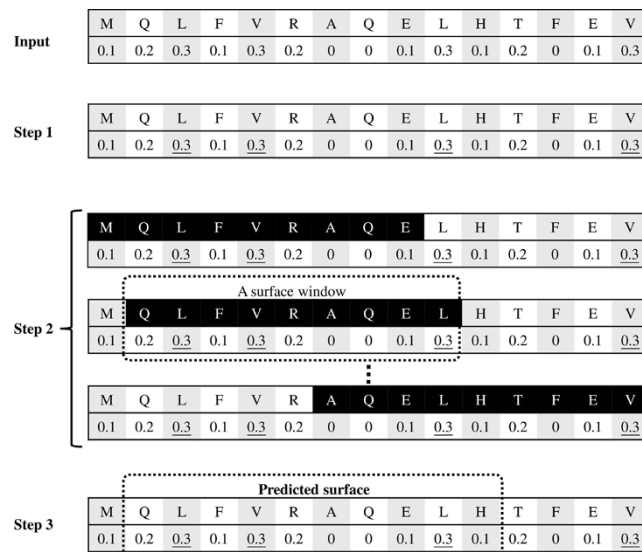


Figure 4
Identifying surface of protein sequence. Input: Each residue of the sequence is associated with a predicted RSA value. Step 1: Identify surface residues having RSA values $\geq t$. Step 2: Scan the sequence with a sliding window of size w , where each surface window must include at least o surface residues. Step 3: Predicted surface is union of all surface windows. $t = 0.3$, $w = 9$ and $o = 3$ in this example.

the protein sequence. A sliding window is identified as a surface window if it contains at least o surface residues. Finally, the predicted surface is the union of all surface windows. In this study, t and w are parameters to be set either by cross-validation or by the user, while o is suggested to be three according to the experiment results.

Feature encoding

Based on the design by Shen *et al.* [24], this work encodes each protein sequence as a feature vector by considering the frequencies of conjoint triads of that protein sequence. An amino acid triad regards is a unit of three continuous amino acids. Each PPI pair is thus encoded by concatenating the two feature vectors of the two individual proteins of that pair. The 20 amino acids are clustered into seven groups (Table 6) based on their dipoles and side chain volumes.

Figure 5 depicts the process of encoding a protein sequence. First, the protein sequence is transformed into

Table 6: Amino acid groups used herein

Group no.	Amino acids
1	Ala, Gly, Val
2	Ile, Leu, Phe, Pro
3	Tyr, Met, Thr, Ser
4	His, Asn, Gln, Tpr
5	Arg, Lys
6	Asp, Glu
7	Cys

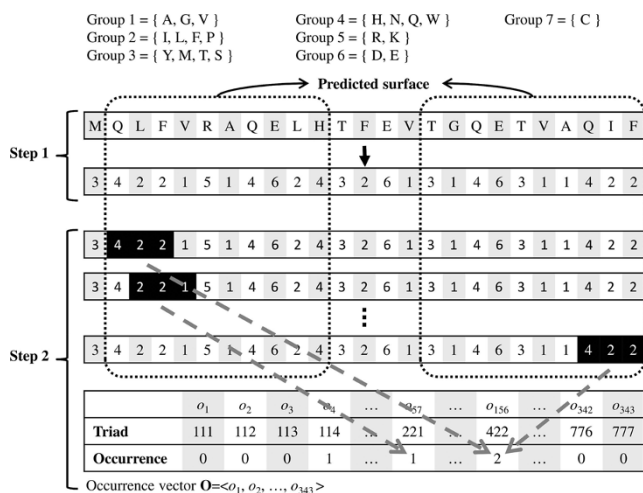


Figure 5
Encoding a protein sequence as a feature vector using conjoint triads. Step 1: Transform the amino acid sequence into the group sequence. Step 2: Scan the predicted surface along the group sequence, and count the triads in the occurrence vector \mathbf{O} .

a group sequence. This method then scans the predicted surface along the group sequence. Each scanned triad is counted in an occurrence vector, \mathbf{O} , of which each element o_i represents the number of the i -th type of triad observed in the predicted surface. The major contribution of this work is to ignore the occurrences of conjoint triads outside the predicted surface. The two vectors of both sequences of a pair of proteins are concatenated to form a 686-dimensional feature vector.

Relaxed variable kernel density estimator

The relaxed variable kernel density estimator (RVKDE) [25] is used as the classification tool for PPI prediction. A kernel density estimator is in fact an approximate probability density function. Let $\{s_1, s_2, \dots, s_n\}$ be a set of sampling instances randomly and independently taken from the distribution governed by f_X in the m -dimensional vector space. Then, with the RVKDE algorithm, the value of f_X at point \mathbf{v} is estimated as follows:

$$\hat{f}(\mathbf{v}) = \frac{1}{|n|} \sum_{s_i} \left(\frac{1}{\sqrt{2\pi} \cdot \sigma_i} \right)^m \exp \left(-\frac{\|\mathbf{v} - s_i\|^2}{2\sigma_i^2} \right), \text{ where}$$

- 1) $\sigma_i = \beta \frac{R(s_i)\sqrt{\pi}}{n^{1/(k+1)}\Gamma(\frac{m}{2}+1)}$;
- 2) $R(s_i)$ is the maximum distance between s_i and its k s nearest training instances;
- 3) $\Gamma(\cdot)$ is the Gamma function [48];
- 4) β and k s are parameters to be set either through cross-validation or by the user.

When using RVKDE to predict protein-protein interactions, two kernel density estimators are constructed to approximate the distribution of interacting and non-interacting protein pairs, respectively. A query protein pair (represented as the feature vector \mathbf{v}) is predicted to the class that gives the maximum value among the two likelihood functions defined as follows:

$$L_j(\mathbf{v}) = \frac{|S_j| \cdot \hat{f}_j(\mathbf{v})}{\sum_h |S_h| \cdot \hat{f}_h(\mathbf{v})}$$

where $|S_j|$ is the number of class- j training instances, and $\hat{f}_j(\mathbf{v})$ is the kernel density estimator corresponding to class- j training instances. In this study, j is either 'interacting' or 'non-interacting'. Current RVKDE implementation includes only a limited number, denoted by kt , of the nearest class- j training instances of \mathbf{v} while computing $\hat{f}_j(\mathbf{v})$ in order to improve the efficiency of

the predictor. The *kt* is also a parameter to be set either through cross-validation or by the user.

Competing interests

The authors declare that they have no competing interests.

Authors' contributions

Author DTHC designed the methodology and conceived of this study. YTS and BCL designed the experiments and performed all calculations and analyses. All authors have read and approved this manuscript.

Acknowledgements

The authors would like to thank the National Science Council of the Republic of China, Taiwan, for financially supporting this research under Contract Nos. NSC 97-2627-P-001-002, NSC 96-2320-B-006-027-MY2 and NSC 96-2221-E-006-232-MY2. Ted Knoy is appreciated for his editorial assistance.

This article has been published as part of *BMC Bioinformatics* Volume 11 Supplement 1, 2010: Selected articles from the Eighth Asia-Pacific Bioinformatics Conference (APBC 2010). The full contents of the supplement are available online at <http://www.biomedcentral.com/1471-2105/11?issue=S1>.

References

- Ge H, Walhout AJM and Vidal M: **Integrating 'omic' information: a bridge between genomics and systems biology.** *Trends Genet* 2003, **19(10)**:551–560.
- Ito T, Chiba T, Ozawa R, Yoshida M, Hattori M and Sakaki Y: **A comprehensive two-hybrid analysis to explore the yeast protein interactome.** *Proc Natl Acad Sci USA* 2001, **98(8)**:4569–4574.
- Ho Y, Gruhler A, Heilbut A, Bader GD, Moore L, Adams SL, Millar A, Taylor P, Bennett K and Boutilier K, et al: **Systematic identification of protein complexes in *Saccharomyces cerevisiae* by mass spectrometry.** *Nature* 2002, **415(6868)**:180–183.
- Gavin AC, Aloy P, Grandi P, Krause R, Boesche M, Marzioch M, Rau C, Jensen LJ, Bastuck S and Dumpelfeld B, et al: **Proteome survey reveals modularity of the yeast cell machinery.** *Nature* 2006, **440(7084)**:631–636.
- Tong AHY, Drees B, Nardelli G, Bader GD, Brannetti B, Castagnoli L, Evangelista M, Ferracuti S, Nelson B and Paoluzi S, et al: **A combined experimental and computational strategy to define protein interaction networks for peptide recognition modules.** *Science* 2002, **295(5553)**:321–324.
- Han JDJ, Dupuy D, Bertin N, Cusick ME and Vidal M: **Effect of sampling on topology predictions of protein-protein interaction networks.** *Nat Biotechnol* 2005, **23(7)**:839–844.
- Hart GT, Ramani AK and Marcotte EM: **How complete are current yeast and human protein-interaction networks.** *Genome Biol* 2006, **7(11)**:120.
- Shoemaker BA and Panchenko AR: **Deciphering protein-protein interactions. Part II. Computational methods to predict protein and domain interaction partners.** *PLoS Comput Biol* 2007, **3(4)**:e43.
- Pellegrini M, Marcotte EM, Thompson MJ, Eisenberg D and Yeates TO: **Assigning protein functions by comparative genome analysis: Protein phylogenetic profiles.** *Proc Natl Acad Sci USA* 1999, **96(8)**:4285–4288.
- Aloy P and Russell RB: **InterPreTS: protein Interaction Prediction through Tertiary Structure.** *Bioinformatics* 2003, **19(1)**:161–162.
- Ogmen U, Keskin O, Aytuna AS, Nussinov R and Gursoy A: **PRISM: protein interactions by structural matching.** *Nucleic Acids Res* 2005, **33**:W331–W336.
- Enright AJ, Iliopoulos I, Kyripides NC and Ouzounis CA: **Protein interaction maps for complete genomes based on gene fusion events.** *Nature* 1999, **402(6757)**:86–90.
- Marcotte EM, Pellegrini M, Ng HL, Rice DW, Yeates TO and Eisenberg D: **Detecting protein function and protein-protein interactions from genome sequences.** *Science* 1999, **285(5428)**:751–753.
- Huang TW, Tien AC, Lee YCG, Huang WS, Lee YCG, Peng CL, Tseng HH, Kao CY and Huang CYF: **POINT: a database for the prediction of protein-protein interactions based on the orthologous interactome.** *Bioinformatics* 2004, **20(17)**:3273–3276.
- Espadaler J, Romero-Isart O, Jackson RM and Oliva B: **Prediction of protein-protein interactions using distant conservation of sequence patterns and structure relationships.** *Bioinformatics* 2005, **21(16)**:3360–3368.
- Valencia A and Pazos F: **Computational methods for the prediction of protein interactions.** *Curr Opin Struct Biol* 2002, **12(3)**:368–373.
- Ben-Hur A and Noble WS: **Kernel methods for predicting protein-protein interactions.** *Bioinformatics* 2005, **21**:138–146.
- Chen XW and Liu M: **Prediction of protein-protein interactions using random decision forest framework.** *Bioinformatics* 2005, **21(24)**:4394–4400.
- Martin S, Roe D and Faulon JL: **Predicting protein-protein interactions using signature products.** *Bioinformatics* 2005, **21(2)**:218–226.
- Chou KC and Cai YD: **Predicting protein-protein interactions from sequences in a hybridization space.** *J Proteome Res* 2006, **5(2)**:316–322.
- Pitre S, Dehne F, Chan A, Cheatham J, Duong A, Emili A, Gebbia M, Greenblatt J, Jessulat M and Krogan N, et al: **PIPE: a protein-protein interaction prediction engine based on the re-occurring short polypeptide sequences between known interacting protein pairs.** *BMC Bioinformatics* 2006, **7**.
- Shen JW, Zhang J, Luo XM, Zhu WL, Yu KQ, Chen KX, Li YX and Jiang HL: **Predicting protein-protein interactions based only on sequence information.** *Proc Natl Acad Sci USA* 2007, **104(11)**:4337–4341.
- Guo YZ, Yu LZ, Wen ZN and Li ML: **Using support vector machine combined with auto covariance to predict protein-protein interactions from protein sequences.** *Nucleic Acids Res* 2008, **36(9)**:3025–3030.
- Shen JW, Zhang J, Luo XM, Zhu WL, Yu KQ, Chen KX, Li YX and Jiang HL: **Predicting protein-protein interactions based only on sequence information.** *Proceedings of the National Academy of Sciences of the United States of America* 2007, **104(11)**:4337–4341.
- Oyang YJ, Hwang SC, Ou YY, Chen CY and Chen ZW: **Data classification with radial basis function networks based on a novel kernel density estimation algorithm.** *IEEE Transactions on Neural Networks* 2005, **16(1)**:225–236.
- Chang DTH, Huang HY, Syu YT and Wu CP: **Real value prediction of protein solvent accessibility using enhanced PSSM features.** *BMC Bioinformatics* 2008, **9(Suppl 12)**:S12.
- Kirchmair J, Markt P, Distinto S, Schuster D, Spitzer GM, Liedl KR, Langer T and Wolber G: **The Protein Data Bank (PDB), Its Related Services and Software Tools as Key Components for In Silico Guided Drug Discovery.** *Journal of Medicinal Chemistry* 2008, **51(22)**:7021–7040.
- Dohkan S, Koike A and Takagi T: **Improving the Performance of an SVM-Based Method for Predicting Protein-Protein Interactions.** *In Silico Biol* 2006, **6**:515–529.
- Zhu J, Zhang B, Smith EN, Drees B, Brem RB, Kruglyak L, Bumgarner RE and Schadt EE: **Integrating large-scale functional genomic data to dissect the complexity of yeast regulatory networks.** *Nat Genet* 2008, **40(7)**:854–861.
- Nielsen J and Oliver S: **The next wave in metabolome analysis.** *Trends Biotechnol* 2005, **23(11)**:544–546.
- Rajagopalan D and Agarwal P: **Inferring pathways from gene lists using a literature-derived network of biological relationships.** *Bioinformatics* 2005, **21(6)**:788–793.
- Cherry JM, Adler C, Ball C, Chervitz SA, Dwight SS, Hester ET, Jia YK, Juvi G, Roe T and Schroeder M, et al: **SGD: *Saccharomyces Genome Database*.** *Nucleic Acids Research* 1998, **26(1)**:73–79.
- Zhu J and Zhang MQ: **SCPD: a promoter database of the yeast *Saccharomyces cerevisiae*.** *Bioinformatics* 1999, **15(7-8)**:607–611.
- Wingender E, Chen X, Fricke E, Geffers R, Hehl R, Liebich I, Krull M, Matsys V, Michael H and Ohnhauser R, et al: **The TRANSFAC**

- system on gene expression regulation. *Nucleic Acids Research* 2001, **29(1)**:281–283.
35. Mewes HW, Frishman D, Guldener U, Mannhaupt G, Mayer K, Mokrejs M, Morgenstern B, Munsterkotter M, Rudd S and Weil B: **MIPS: a database for genomes and protein sequences.** *Nucleic Acids Research* 2002, **30(1)**:31–34.
 36. Bairoch A, Consortium U, Bougueleret L, Altairac S, Amendolia V, Auchincloss A, Argoud-Puy G, Axelsen K, Baratin D and Blatter MC, et al: **The Universal Protein Resource (UniProt) 2009.** *Nucleic Acids Research* 2009, **37**:D169–D174.
 37. Kabsch W and Sander C: **Dictionary of Protein Secondary Structure - Pattern-Recognition of Hydrogen-Bonded and Geometrical Features.** *Biopolymers* 1983, **22(12)**:2577–2637.
 38. Nelson DL, Lehninger AL and Cox MM: *Lehninger principles of biochemistry* New York: W.H. Freeman; 52008.
 39. Kim WK and Ison JC: **Survey of the geometric association of domain-domain interfaces.** *Proteins* 2005, **61(4)**:1075–1088.
 40. Kim WK, Henschel A, Winter C and Schroeder M: **The many faces of protein-protein interactions: A compendium of interface geometry.** *Plos Computational Biology* 2006, **2(9)**:e124.
 41. Lise S, Walker-Taylor A and Jones DT: **Docking protein domains in contact space.** *Bmc Bioinformatics* 2006, **7**.
 42. Jones S and Thornton JM: **Principles of protein-protein interactions.** *Proceedings of the National Academy of Sciences of the United States of America* 1996, **93(1)**:13–20.
 43. Altschul SF, Madden TL, Schaffer AA, Zhang JH, Zhang Z, Miller W and Lipman DJ: **Gapped BLAST and PSI-BLAST: a new generation of protein database search programs.** *Nucleic Acids Res* 1997, **25(17)**:3389–3402.
 44. Nam JW, Shin KR, Han JJ, Lee Y, Kim VN and Zhang BT: **Human microRNA prediction through a probabilistic co-learning model of sequence and structure.** *Nucleic Acids Res* 2005, **33(11)**:3570–3581.
 45. Nguyen MN and Rajapakse JC: **Two-stage support vector regression approach for predicting accessible surface areas of amino acids.** *Proteins* 2006, **63(3)**:542–550.
 46. Witten IH and Frank E: **Data mining: practical machine learning tools and techniques.** Amsterdam; Boston, MA: Morgan Kaufman; 22005.
 47. Chang CC and Lin Cj: **LIBSVM: a library for support vector machines.** 2001 <http://www.csie.ntu.edu.tw/~cjlin/libsvm>.
 48. Artin E: **The Gamma Function.** New York: Holt, Rinehart and Winston; 1964.

Publish with **BioMed Central** and every scientist can read your work free of charge

"BioMed Central will be the most significant development for disseminating the results of biomedical research in our lifetime."

Sir Paul Nurse, Cancer Research UK

Your research papers will be:

- available free of charge to the entire biomedical community
- peer reviewed and published immediately upon acceptance
- cited in PubMed and archived on PubMed Central
- yours — you keep the copyright

Submit your manuscript here:
http://www.biomedcentral.com/info/publishing_adv.asp

